

# Sitatapatra: Blocking the Transfer of Adversarial Samples

Ilia Shumailov<sup>\*1</sup> Xitong Gao<sup>\*2</sup> Yiren Zhao<sup>\*1</sup> Robert Mullins<sup>1</sup> Ross Anderson<sup>1</sup> Cheng-Zhong Xu<sup>2</sup>

## Abstract

Convolutional Neural Networks (CNNs) are widely used to solve classification tasks in computer vision. However, they can be tricked into misclassifying specially crafted “adversarial” samples – and samples built to trick one model often work alarmingly well against other models trained on the same task. In this paper we introduce Sitatapatra, a system designed to block the transfer of adversarial samples. It diversifies neural networks using a key, as in cryptography, and provides a mechanism for detecting attacks. What’s more, when adversarial samples are detected they can typically be traced back to the individual device that was used to develop them. The run-time overheads are minimal permitting the use of Sitatapatra on constrained systems.

## 1. Introduction

Convolutional Neural Networks (CNNs) have achieved revolutionary performance in vision-related tasks such as segmentation (Badrinarayanan et al., 2015), image classification (Krizhevsky et al., 2012), object detection (Ren et al., 2015) and visual question answering (Antol et al., 2015). It is now inevitable that CNNs will be deployed widely for a broad range of applications including both safety-critical and security-critical tasks such as autonomous vehicles (Fang et al., 2003), face recognition (Schroff et al., 2015) and action recognition (Ji et al., 2013).

However, researchers have discovered that small perturbations to input images can trick CNNs — with classifiers producing results surprisingly far from the correct answer in response to small perturbations that are not perceptible by humans. An attacker can thus create adversarial image inputs that cause a CNN to misbehave. The resulting attack

scenarios are broad, ranging from breaking into smartphones through face-recognition systems (Carlini et al., 2016) to misdirecting autonomous vehicles through perturbed road signs (Eykholt et al., 2018).

The attacks are also practical, because they are surprisingly portable. If devices are shipped with the same CNN classifier, the attacker only needs to analyze a single one of them to perform effective attacks on the others. Imagine a firm that deploys the same CNN on devices in very different environments. An attacker might not be able to experiment with a security camera in a bank vault, but if a cheaper range of security cameras are sold for home use and use the same CNN, he may buy one and generate transferable adversarial samples using it. And making CNNs sufficiently different is not straightforward. Recent research teaches that different CNNs trained to solve similar problems are often vulnerable to the same adversarial samples (Papernot et al., 2016a; Zhao et al., 2018b).

It is clear that we need an efficient way of limiting the transferability of adversarial samples. And given the complexity of the scenarios in which sensors operate, the protection mechanism should: *a)* work in computationally constrained environments; *b)* require minimal changes to the model architecture, and; *c)* offer a way of building complex security policies.

In this paper we propose Sitatapatra, a system designed and built to constrain the transferability of adversarial examples. Inspired by cryptography, we introduce a *key* into CNNs that causes each network of the same architecture to be internally different enough to stop the transferability of adversarial attacks. We describe multiple ways of embedding the *keys* and evaluate them extensively on a range of computer vision benchmarks. Based on these data, we propose a scheme to pick *keys*. Finally, we discuss the scalability of the Sitatapatra defence and describe the trade-offs inherent in its design.

The contributions of this paper are:

- We introduce Sitatapatra, the first system designed to stop adversarial samples being transferable.
- We describe how to embed a secret *key* into CNNs.
- We show that Sitatapatra not only blocks sample trans-

<sup>\*</sup>Equal contribution <sup>1</sup>Computer Laboratory, University of Cambridge <sup>2</sup>Shenzhen Institutes of Advanced Technology, Shenzhen, China. Correspondence to: Yiren Zhao <yiren.zhao@cl.cam.ac.uk>, Ilia Shumailov <ilia.shumailov@cl.cam.ac.uk>, Xitong Gao <xt.gao@siat.ac.cn>.

fer, but also allows detection and attack attribution.

- We measure performance and show that the run-time computational overhead is low enough (0.6–7%) for Sitatapatra to work on constrained devices.

The paper is structured as follows. Section 2 describes the related work. Section 3 introduces the methodology of Sitatapatra and presents the design choices. Section 4 evaluates the system against state-of-the-art attacks on three popular image classification benchmarks. Section 5 discusses the trade-offs in Sitatapatra, analyses *key* diversity and the costs of *key* change, and discusses how to deploy Sitatapatra effectively at scale.

## 2. Related Work

Since the invention of adversarial attacks against CNNs (Szegedy et al., 2013), there has been rapid co-evolution of attack and defense techniques in the deep learning community.

An adversarial sample is defined as a slightly perturbed image  $\hat{\mathbf{x}}$  of the original  $\mathbf{x}$ , while  $\hat{\mathbf{x}}$  and  $\mathbf{x}$  are assigned different classes by a CNN classifier  $F$ . The  $l^p$ -norm of the perturbation is often constrained by a small constant  $\epsilon$  such that  $\|\hat{\mathbf{x}} - \mathbf{x}\|_p \leq \epsilon$  and  $0 \leq \hat{\mathbf{x}} \leq 1$ , where  $p$  can be 1, 2, or  $\infty$ .

The fast gradient sign method (FGSM) (Goodfellow et al., 2015) is a simple and effective  $L^\infty$  attack for finding such samples. FGSM generates  $\hat{\mathbf{x}}$  by computing the gradient of the target class  $y$  with respect to  $\mathbf{x}$ , and applies a distortion  $\epsilon$  for all pixels against the sign of the gradient direction:

$$\hat{\mathbf{x}} = \text{clip}(\mathbf{x} + \epsilon \cdot \text{sign}(\nabla_{\mathbf{x}} \ell_y(F(\mathbf{x}))), \quad (1)$$

where  $\ell_y(F(\mathbf{x}))$  denotes the loss of the network output  $F(\mathbf{x})$  for the target class  $y$ ,  $\nabla_{\mathbf{x}}(\mathbf{z})$  evaluates the gradient of  $\mathbf{z}$  with respect to  $\mathbf{x}$ , the sign function returns the signs  $\{\pm 1\}$  of the values in its input tensor, and finally  $\text{clip}(\mathbf{z}) = \max(\min(\mathbf{z}, 1), 0)$  constraints each value to the range of permissible pixel values, *i.e.*  $[0, 1]$ .

DeepFool (Moosavi-Dezfooli et al., 2016) is an attack that iteratively linearizes misclassification boundaries of the network, and perturbs the image by moving along the direction that gives the nearest misclassification.

The Carlini & Wagner attack (Carlini & Wagner, 2017) formulates the following optimization problem, whose solution gives an adversarial sample:

$$\min_{\mathbf{x}^*} \|\mathbf{x}^* - \mathbf{x}\|_2^2 + c \cdot G(\mathbf{x}^*). \quad (2)$$

Here, the first term optimizes the  $L^2$ -distance, while the second term  $G(\mathbf{x}^*) = \max(\{-\kappa\} \cup \{\ell_{y'}(\mathbf{z}) - \ell_y(\mathbf{z}) \mid y' \neq y, \mathbf{z} = F(\mathbf{x}^*)\})$  minimizes the loss of classes other than  $y$ , and  $\kappa$  controls the confidence of misclassification.

Furthermore, it is well-known that adversarial samples demonstrate good transferability (Szegedy et al., 2013; Goodfellow et al., 2015; Liu et al., 2017), *i.e.* such samples generated from a model  $F$  tend to remain adversarial for models other than  $F$ . This is problematic as black-box attacks may generate strong adversarial inputs, without even requiring any prior knowledge on the architecture and training procedures of the model under attack (Papernot et al., 2017). Table 1 shows that exact scenario — adversarial samples generated from one model can effectively transfer to another with the same architecture trained only with different initializations.

Many researchers have proposed defences based on changes to the network architecture or the training procedure. Random self-ensemble (Liu et al., 2018) adds noise to computed features to simulate a random ensemble of models. Deep Defence (Yan et al., 2018) incorporates the perturbation required to generate adversarial samples as a regularization during training, thus making the trained model less susceptible to adversarial samples. Other methods such as adversarial training (Goodfellow et al., 2015), defensive distillation (Papernot et al., 2016b) and Bayesian neural networks (Liu et al., 2019), also demonstrate good resistance against adversarial samples. The above methods can produce robust models with greater attack resistance, yet this is often at the cost of the original model’s accuracy (Tsipras et al., 2019). For this reason, many other researchers extended the networks to detect adversarial attacks explicitly (Metzen et al., 2017; Meng & Chen, 2017; Shumailov et al., 2018), but some of these detection methods can add considerable computational overhead.

## 3. Method

### 3.1. High-Level View

We start with a high-level description of our method. Each convolutional layer with ReLU activation is sequentially extended with a guard (Figure 1b) and a detector (Figure 1a) layer. Intuitively, the guard encourages the gradient to disperse among differently initialized models, limiting sample transferability. If this fails, the detector works as our second line of defence by raising an alarm at potentially adversarial samples. The rest of this section explains the design of the two modules, which work in tandem or individually to defend against and/or detect most instances of the adversarial attacks considered here.

### 3.2. Static Channel Manipulation

Where an attack sample is transferable, we hypothesize that by moving along the gradient direction of the input image that gave rise to the adversarial sample, some of the neurons of the network are likely to be highly excited.

	Params	LeNet5					MCifarNet					ResNet18-Cifar10					ResNet18-Cifar100				
		$S_{Acc}(\%)$	$T_{Acc}(\%)$	$\Delta_{Acc}(\%)$	$l_2$	$l_\infty$	$S_{Acc}(\%)$	$T_{Acc}(\%)$	$\Delta_{Acc}(\%)$	$l_2$	$l_\infty$	$S_{Acc}(\%)$	$T_{Acc}(\%)$	$\Delta_{Acc}(\%)$	$l_2$	$l_\infty$	$S_{Acc}(\%)$	$T_{Acc}(\%)$	$\Delta_{Acc}(\%)$	$l_2$	$l_\infty$
Clean		99.13	99.25	-	-	-	89.51	90.14	-	-	-	91.12	93.58	-	-	-	71.69	72.04	-	-	-
FGSM	$\epsilon = 0.02$	98.20	98.91	0.70	0.42	0.02	17.03	24.22	7.19	0.98	0.02	18.05	50.16	32.11	0.99	0.02	12.97	36.64	23.67	0.76	0.01
	$\epsilon = 0.06$	92.19	96.17	3.98	1.65	0.08	2.89	11.17	8.28	3.67	0.07	4.61	22.66	18.05	3.71	0.07	2.50	15.08	12.58	2.92	0.05
	$\epsilon = 0.6$	0.55	3.59	3.05	11.91	0.59	1.02	7.81	6.80	20.98	0.48	0.00	8.59	8.59	22.07	0.50	0.16	8.67	8.52	18.11	0.42
	mean	-	-	2.58	-	-	-	-	7.42	-	-	-	-	19.58	-	-	-	-	14.92	-	-
DeepFool	$i = 50$	14.92	92.03	77.11	1.86	0.44	1.02	27.34	26.33	0.20	0.03	1.02	88.20	87.19	0.16	0.02	1.95	67.34	65.39	0.08	0.01
	$i = 10$	87.73	96.95	9.22	1.76	0.41	1.80	27.34	25.55	0.20	0.03	1.72	88.20	86.48	0.16	0.02	3.20	67.34	64.14	0.08	0.01
	mean	-	-	43.17	-	-	-	-	25.94	-	-	-	-	86.84	-	-	-	-	64.77	-	-
C&W	$lr = 0.5$	3.75	86.56	82.81	3.09	0.71	2.03	10.47	8.44	9.86	0.24	0.55	15.00	14.45	10.02	0.24	0.55	10.47	9.92	7.14	0.18
	$lr = 1.0$	1.02	60.86	59.84	4.25	0.76	5.00	11.02	6.02	17.28	0.44	0.62	12.81	12.19	17.75	0.45	0.70	9.22	8.52	12.88	0.33
	mean	-	-	71.33	-	-	-	-	7.23	-	-	-	-	13.32	-	-	-	-	9.22	-	-
C&W	$lr = 0.5$	3.91	15.78	11.88	5.12	0.90	2.73	4.69	1.95	15.89	0.52	1.09	10.39	9.30	14.63	0.43	0.86	1.48	0.62	13.77	0.42
	$c = 0.999$	1.09	6.17	5.08	5.75	0.95	5.47	5.23	-0.23	24.27	0.77	1.48	8.83	7.34	25.35	0.81	0.78	1.41	0.62	19.89	0.55
	mean	-	-	8.48	-	-	-	-	0.86	-	-	-	-	8.32	-	-	-	-	0.62	-	-
Mean		-	-	27.09	-	-	-	-	9.21	-	-	-	-	28.46	-	-	-	-	19.90	-	-

Table 1. Transferability of two pretrained models with different initializations on various datasets. Source and Target are two models of the same topology but different initialization point.  $\epsilon$  is a hyperparameter in FGSM,  $i$  is the number of iterations and  $lr$  is the learning rate.  $c$  is the confidence, the adversarial sample has to cause the misclassified class to have a probability above this given threshold.

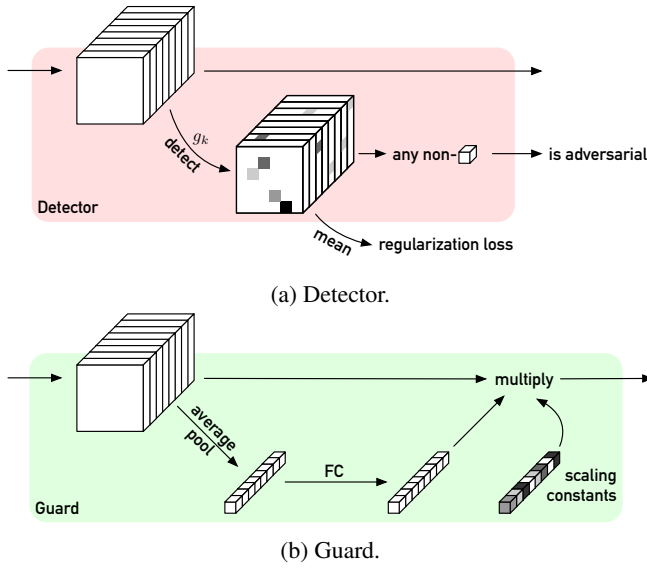


Figure 1. High-level view of the module extensions we add to networks to stop and detect transferred adversarial samples.

By monitoring abnormal excitation, we can detect many adversarial samples.

In Sitatapatra, we use a simple concept – we train neural networks using the original datasets, but with additional activation regularization, so that a certain set of outputs, and of intermediate activation values, are not generated by any of the training set inputs. If one of these ‘taboo’ activations is observed, this serves as a signal that the input may be adversarial, and as different instances of the model can be trained with different taboo sets, we have a way to introduce diversity that is analogous to the *keys* used in cryptographic systems. This approach is much faster than, for example, adversarial training (Goodfellow et al., 2015). By regularizing the activation feature maps, clean samples yield well-bounded activation results, yet adversarial ones typically result in highly excited neuron outputs in activa-

tions (Shumailov et al., 2018). Using this, we can design our detector (Figure 1a) so that uncompromised models can successfully block most adversarial samples transferred from compromised models, even under the strong assumption that the models share the same network architecture and dataset.

For simplicity, we consider a feed-forward CNN  $F$  consisting of a sequence of  $L$  convolutional layers, where the  $l^{\text{th}}$  layer computes output feature maps  $\mathbf{x}_l \in \mathbb{R}^{C_l \times H_l \times W_l}$ . Here,  $\mathbf{x}_l$  is a collection of feature maps with  $C_l$  channels of  $H_l \times W_l$  images, where  $H_l$  and  $W_l$  respectively denote the width and height of the image.

The detector module additionally performs the following polynomial transformation  $f_k$  to the features of each layer output, which can be derived from the *key* of the network:

$$f_k(\mathbf{x}_l) = a_n \mathbf{x}_l^n + a_{n-1} \mathbf{x}_l^{n-1} + \dots + a_0, \quad (3)$$

and the transformation is then followed by the following criterion evaluation:

$$g_k(\mathbf{x}_l) = f_k(\mathbf{x}_l) \cdot (\text{sign}(f_k(\mathbf{x}_l) - t))_+. \quad (4)$$

Here,  $\cdot$  is element-wise multiplication,  $(\mathbf{z})_+ = \max(0, \mathbf{z})$  denotes the ReLU activation, the degrees of the polynomial  $n$  and the constant values  $a_0, a_1, \dots, a_n$  and  $t > 0$  can be identified as the *key* embedded into the network. During training with clean dataset samples, any values  $f_k(\mathbf{x}_l) > t$  are penalized, with the following regularization term:

$$\mathcal{R}(\mathbf{x}) = \sum_{l \in L} \|g_k(\mathbf{x}_l)\|_1. \quad (5)$$

As we will examine closely in Section 4, the  $g_k(\mathbf{x}_l)$  evaluated from adversarial samples generally produce positive results, whereas clean validation samples usually do not trigger this criterion. Our detector uses of this to identify adversarial samples. In addition, the polynomial can be

evaluated efficiently with Horner’s method (Knuth, 1962), requiring only  $n$  multiply-accumulate operations per value, which is insignificant when compared to the computational cost of the convolutions. Finally, the non-linear nature of our regularization diversifies the weight distributions among models, which intuitively explains why adversarial samples become less likely to transfer.

### 3.3. Dynamic Channel Manipulation

In this section, we present the design of the guard module. It dynamically manipulates feature maps using per-channel attention, which is in turn inspired by the squeeze-excitation networks (Hu et al., 2017) and feature boosting (Gao et al., 2019). As with the detector modules described earlier in Section 3.2, we extend existing networks by adding a guard module immediately after each convolutional layer and its detector module. The  $l^{\text{th}}$  module accepts  $\mathbf{x}_l$  computed by the previous convolutional layer as its input, and introduces a small auxiliary network  $h : \mathbb{R}^{C_l \times H_l \times W_l} \rightarrow \mathbb{R}^{C_l \times H_l \times W_l}$ , which amplifies important channels and suppresses unimportant ones in feature maps, before feeding the results of  $h(\mathbf{x}_l)$  to the next convolutional layer. The auxiliary network is illustrated in Figure 1b and is defined as:

$$h(\mathbf{x}_l) = \mathbf{x}_l \cdot (\gamma_l \cdot \text{pool}(\mathbf{x}_l) \phi_l), \quad (6)$$

where  $\text{pool} : \mathbb{R}^{C_l \times H_l \times W_l} \rightarrow \mathbb{R}^{C_l}$  performs a global average pool on the feature maps  $\mathbf{x}_l$  which reduces them to a vector of  $C_l$  values,  $\phi \in \mathbb{R}^{C_l \times C_l}$  is a matrix of trainable parameters, and  $\cdot$  denotes element-wise multiplication between tensors which broadcasts in a channel-wise manner. Finally,  $\gamma_l$  is a vector of  $C_l$  scaling constants, where each value is randomly drawn from a uniform distribution between 0 and 1, using the crypto-key embedded within the model as the random seed. By doing so, each deployed model can have a different  $\gamma_l$  value, which diversifies the gradients among models and forces the fine-tuned models to adopt different local minima.

We will next report how well the guard module can prevent the transfer of adversarial samples.

## 4. Evaluation

### 4.1. Networks, Datasets and Attacks

We evaluate Sitatapatra on three datasets: MNIST (LeCun et al., 2010), CIFAR10 and CIFAR100 (Krizhevsky et al., 2014). In MNIST, we use the LeNet5 architecture (LeCun et al., 2015). In CIFAR10, we use an efficient CNN architecture (MCifarNet) from Mayo (Zhao et al., 2018a) that achieved a high classification rate using only 1.3M parameters. ResNet18 and ResNet34 are also considered on the CIFAR10 and CIFAR100 datasets (He et al., 2016).

We evaluated the performance of clean networks and Si-

tatapatra networks, using two clean models with different initializations as the baseline. For the Sitatapatra models we had two different keys applied on the source and target models. The keys used are  $2x^2 + 3x + 5 < 6$  and  $0.1x^2 - x + 2 < 3$  respectively. The choice is keys will be analyzed later in Section 5.

### 4.2. Static Channel Manipulation

We show the effects of applying only static channel manipulation (SCM) on LeNet5 and MCifarNet in Table 2. For models that are instrumented with SCM, we make sure the detection rate on an unseen evaluation dataset stays below 1%, which implies the false positive rate stays below 1%. In comparison to the baseline shown in Table 1, we observe a significant increase in accuracies when models are attacked by C&W. In the table we present two versions of Carlini & Wagner (C&W) – first, one that picks the smallest perturbation for the given parameters and second, one that also required the misclassified class to produce a confidence of 99.9% ( $c = 0.999$ ).

We have, on average, a 42.77% net increase in  $\Delta_{\text{acc}}$  for LeNet5 and 100% detection rate on MCifarNet. The same phenomenon is shown on C&W without the confidence threshold —  $\Delta_{\text{acc}}$  increased by 19.37% on LeNet5 and a detection rate of 89.1% is observed on MCifarNet. The improvements in accuracies are marginal for FGSM and DeepFool. DeepFool remains a weak adversary in terms of generating transferable adversarial samples. With 50 steps, it gets good attack performance on the source model, but struggles to transfer to the target model even in the baseline case. FGSM is better, especially FGSM  $\epsilon = 0.6$ ; the attack is very transferable on LeNet5 but most of them can be detected on MCifarNet. We attribute this to a much larger number of channels that are available in MCifarNet and result in better detection rate – the proposed method favours with networks that have more channels. Additionally, we observe a relationship between the amount of distortion that the attacks generate for a given model and the achieved detection rate. For instance, MCifarNet under C&W  $c = 0.999$  achieves a high detection rate since the adversarial samples have large distortions (Table 2). However, the detection mechanism provides minimal benefit when distortions are small (MCifarNet on FGSM  $\epsilon = 0.02$ ).

### 4.3. Static and Dynamic Channel Manipulations

Table 3 shows the performance of combined static and dynamic channels manipulation (SDCM) method. During the training phase we tune each model to have less than 1% false positive detection rate on the clean evaluation dataset. The results show good performance on large models, since large models have more channels available for the proposed instrumentations. For ResNet18 on CIFAR10, we can achieve



Params	LeNet5							MCifarNet						
	$S_{Acc}(\%)$	$T_{Acc}(\%)$	$\Delta_{Acc}(\%)$	$T_{Det}(\%)$	$l_2$	$l_\infty$		$S_{Acc}(\%)$	$T_{Acc}(\%)$	$\Delta_{Acc}(\%)$	$T_{Det}(\%)$	$l_2$	$l_\infty$	
Clean	99.13	99.25	-	-	-	-		89.51	90.14	-	-	-	-	
FGSM	$\epsilon = 0.02$	97.58	99.45	1.87	0.00	0.35	0.02	10.70	21.41	10.70	1.41	0.95	0.02	
	$\epsilon = 0.06$	82.58	98.36	15.78	0.00	1.37	0.08	2.27	11.17	8.91	10.47	3.49	0.06	
	$\epsilon = 0.6$	2.89	13.67	10.78	0.19	9.53	0.58	0.78	9.22	8.44	78.63	20.06	0.46	
	mean	-	-	9.48	0.06	-	-	-	-	9.35	30.17	-	-	
DeepFool	$i = 50$	21.09	99.30	78.20	0.00	1.05	0.25	0.23	69.53	69.30	2.49	0.25	0.03	
	$i = 10$	98.44	99.45	1.02	0.00	1.01	0.25	0.39	69.53	69.14	2.49	0.25	0.03	
	mean	-	-	39.61	0.00	-	-	-	-	69.22	2.49	-	-	
C&W	$lr = 0.5$	6.33	97.34	91.02	0.00	3.01	0.70	4.06	11.33	7.27	89.25	9.43	0.24	
	$lr = 1.0$	1.41	91.80	90.39	0.95	3.99	0.79	9.45	14.45	5.00	88.86	16.33	0.41	
	mean	-	-	90.70	0.48	-	-	-	-	6.14	89.10	-	-	
C&W $c = 0.999$	$lr = 0.5$	6.64	64.14	57.50	2.38	4.89	0.92	5.08	3.59	-1.48	100.00	17.95	0.67	
	$lr = 1.0$	1.95	46.95	45.00	6.47	5.53	0.97	10.86	7.50	-3.36	100.00	22.87	0.76	
	mean	-	-	51.25	4.43	-	-	-	-	-2.42	100.00	-	-	
Mean	-	-	-	43.50	1.11	-	-	-	-	19.32	52.62	-	-	

Table 2. Transferability of LeNet5 and MCifarNet with SCM (using Guard only). Source and Target are two models of the same topology but different SCM instrumentations.  $\epsilon$  is a hyperparameter in FGSM,  $i$  is the number of iterations and  $lr$  is the learning rate.

	Params	LeNet5							MCifarNet							ResNet18-Cifar10							ResNet18-Cifar100						
		$S_{Acc}(\%)$	$T_{Acc}(\%)$	$\Delta_{Acc}(\%)$	$T_{Det}(\%)$	$l_2$	$l_\infty$		$S_{Acc}(\%)$	$T_{Acc}(\%)$	$\Delta_{Acc}(\%)$	$T_{Det}(\%)$	$l_2$	$l_\infty$		$S_{Acc}(\%)$	$T_{Acc}(\%)$	$\Delta_{Acc}(\%)$	$T_{Det}(\%)$	$l_2$	$l_\infty$		$S_{Acc}(\%)$	$T_{Acc}(\%)$	$\Delta_{Acc}(\%)$	$T_{Det}(\%)$	$l_2$	$l_\infty$	
Clean		99.13	99.25	-	-	-	-		89.51	90.14	-	-	-	-		91.12	93.58	-	-	-	-		67.75	72.24	-	-	-	-	
FGSM	$\epsilon = 0.02$	98.52	99.45	0.94	0.00	0.43	0.02		29.77	42.27	12.50	0.67	0.99	0.02		38.52	59.92	21.41	0.82	1.03	0.02		13.67	50.70	37.03	0.16	0.72	0.01	
	$\epsilon = 0.06$	89.38	98.52	9.14	0.00	1.72	0.08		20.94	31.41	10.47	0.92	3.71	0.07		23.75	34.84	11.09	4.31	3.92	0.07		3.75	26.56	22.81	1.17	2.81	0.05	
	$\epsilon = 0.6$	1.09	12.11	11.02	22.28	12.22	0.58	0.08		14.30	14.22	82.95	21.49	0.49	0.16		11.80	11.64	91.15	22.47	0.51	0.00		0.00	13.20	76.16	17.32	0.40	
	mean	-	-	7.00	7.43	-	-	-		-	12.40	28.18	-	-	-	-	-	-	14.71	32.09	-	-	-	-	-	24.35	25.83	-	-
DeepFool	$i = 50$	11.48	98.91	87.42	0.00	1.51	0.39		0.23	76.25	76.02	1.30	0.38	0.05		3.75	77.27	73.52	7.63	0.87	0.10		1.33	71.33	70.00	0.00	0.14	0.02	
	$i = 10$	89.61	99.22	9.61	0.00	1.44	0.37		2.97	76.17	73.20	1.30	0.38	0.05		6.33	77.50	71.17	6.95	0.81	0.10		2.58	71.33	68.75	0.00	0.13	0.02	
	mean	-	-	48.52	0.00	-	-	-	-	-	74.61	1.30	-	-	-	-	-	-	72.35	7.29	-	-	-	-	-	68.38	0.00	-	-
C&W	$lr = 0.5$	4.38	93.98	89.61	2.35	2.95	0.66		3.83	11.48	7.66	67.41	9.82	0.25		2.73	20.55	17.81	95.50	10.11	0.25		0.39	16.41	16.02	72.42	6.78	0.17	
	$lr = 1.0$	1.56	80.47	78.91	4.78	3.74	0.75		5.31	13.91	8.59	92.02	17.11	0.43		3.52	11.72	8.20	96.05	17.84	0.46		0.62	13.98	13.36	76.58	12.28	0.31	
	mean	-	-	84.26	3.56	-	-	-	-	-	8.13	79.72	-	-	-	-	-	-	13.01	95.78	-	-	-	-	-	14.69	74.50	-	-
C&W $c = 0.999$	$lr = 0.5$	4.61	29.92	25.31	16.02	5.22	0.94		4.53	4.77	0.23	99.10	17.37	0.61		3.05	15.70	12.66	98.60	12.63	0.38		1.56	2.11	0.55	99.92	15.56	0.50	
	$lr = 1.0$	1.88	14.53	12.66	24.07	5.92	0.98		7.19	7.58	0.39	100.00	23.58	0.80		5.55	8.67	3.12	98.72	22.20	0.72		1.72	0.78	-0.94	100.00	21.76	0.66	
	mean	-	-	18.99	20.05	-	-	-	-	-	0.31	99.55	-	-	-	-	-	-	7.89	98.69	-	-	-	-	-	-0.20	99.96	-	-
Mean		-	-	36.06	7.72	-	-	-	-	-	22.60	49.52	-	-	-	-	-	-	25.63	55.53	-	-	-	-	-	34.13	47.38	-	-

Table 3. Transferability of different models on various datasets with the SDCM instrumentation (Guard and Detector). Source and Target are two models of the same topology but different SDCM instrumentations.  $\epsilon$  is a hyperparameter in FGSM,  $i$  is the number of iterations and  $lr$  is the learning rate.  $c$  is the confidence, the adversarial sample has to cause the misclassified class to have a probability above this given threshold.

above 95% detection of all adversarial samples. Similarly, we believe that the performance increase, in comparison to both LeNet5 and MCifarNet, comes from an increased number of channels of the ResNet18 model. Furthermore, we observe a trade-off between the accuracy difference ( $\Delta_{acc}$ ) and the detection rate ( $T_{det}$ ). When attacks achieve low classification accuracies on the target model, the detector, acting as a second line of defence, usually identifies the adversarial examples.

Further, it can be noticed that the samples that actually transfer well usually result in relatively larger distortions — *e.g.* C&W with high confidence and FGSM 0.6. Although large distortions allow attacks to trick the models, they inevitably trigger the alarm and thus get detected. Meanwhile, attacks with more fine-grained perturbations fail to transfer and the accuracy  $T_{acc}$  remains high. For example, DeepFool consistently shows high  $T_{acc}$  and high  $\Delta_{acc}$ .

Finally, to demonstrate the overall performance of Sitatapatra, we present a comparison between the baseline, SCM and SDCM in Table 4. Both of the proposed methods perform relatively worse for LeNet5, as mentioned before, we believe that this due to the small number of channels at

		Pretrained		Static Only		Combined	
		$\Delta_{Acc}(\%)$		$\Delta_{Acc}(\%)$	$T_{Det}(\%)$	$\Delta_{Acc}(\%)$	$T_{Det}(\%)$
FGSM	$\epsilon = 0.02$	0.70		1.87	0.00	0.94	0.00
	$\epsilon = 0.08$	3.98		15.78	0.00	9.14	0.00
	$\epsilon = 0.6$	3.05		10.78	0.19	11.02	22.28
	mean	2.58		9.48	0.06	7.00	7.43
DeepFool	$i = 50$	77.11		78.20	0.00	87.42	0.00
	$i = 10$	9.22		1.02	0.00	9.61	0.00
	mean	43.17		39.61	0.00	48.52	0.00
C&W	$lr = 0.5$	82.81		91.02	0.00	89.61	2.35
	$lr = 1.0$	59.84		90.39	0.95	78.91	4.78
	mean	71.33		90.70	0.48	84.26	3.56
$c = 0.999$	$lr = 0.5$	11.88		57.50	2.38	25.31	16.02
	$lr = 1.0$	5.08		45.00	6.47	12.66	24.07
	mean	8.48		51.25	4.43	18.99	20.05
Mean		27.09		43.50	1.11	36.06	7.72

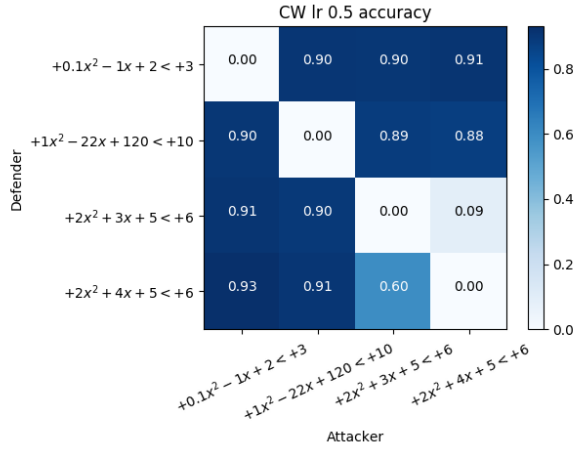
Table 4. Transferability of LeNet5 on MNIST with different instrumentations.  $\Delta_{acc}$  is the difference in accuracies and  $T_{det}$  is the detection rate.  $l_2$  and  $l_\infty$  are the averaged  $l_2$  and  $l_\infty$  norms of the distortions on all input images.  $\epsilon$  is a hyperparameter in FGSM,  $i$  is the number of steps and  $lr$  is learning rate.  $c$  is the confidence, the adversarial sample has to cause the misclassified class to have a probability above this given threshold. We use 20 steps on C&W.

its disposal. Having said that, the proposed methods still greatly outperforms the baseline in terms of  $\Delta_{\text{acc}}$ . The results of DeepFool are very similar across all three methods. DeepFool was not designed with transferability in mind. In contrast, C&W was previously shown to generate highly transferable adversarial samples. The combined method manages to successfully classify the transferred samples and shows sensible detection rates.

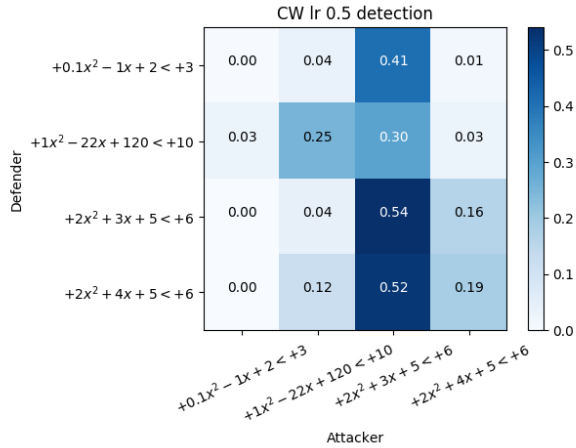
## 5. Discussion

### 5.1. Accuracy, Detection and Computation Overheads

In this section we discuss the trade-offs facing the Sitatapatra user. First and foremost, the choice of keys has an impact on transferability.



(a) Change in Accuracies ( $\Delta_{\text{acc}}$ ).



(b) Detection rates on the target model ( $T_{\text{det}}$ )

Figure 2. Changes in accuracies and detection rates of LeNet5 with various SDCM instrumentations

In Figure 2, we present a confusion matrix with differently instrumented LeNet5 networks attacking each other with

C&W attack for 20 steps and a learning rate of 0.5. The chosen instrumentations are all second-order polynomials, but with different coefficients. It is apparent that Sitatapatra improves the accuracies reported in Figure 2a. However, for the two polynomials,  $2x^2 + 3x + 5 < 6$  and  $2x^2 + 4x + 5 < 6$ , the behavior is different. When using the adversarial samples from  $2x^2 + 4x + 5 < 6$  to attack  $2x^2 + 3x + 5 < 6$ , there is almost zero change in accuracy between the source and the target model, but this relationship does not hold in reverse. The above phenomenon indicates that the adversarial samples generated from one polynomial are transferable to the other when the polynomials are too similar. The same effect is observed in the detector shown in Figure 2b: it is easier to detect adversarial samples from  $2x^2 + 4x + 5 < 6$  to attack  $2x^2 + 3x + 5 < 6$ .

This indicates that, when the models get regularized to polynomials that are similar, the attacks between them end up being transferable. Fortunately, the detection rates remain relatively high even in this case. Different polynomials restrict the activation value range in different ways. In practice, we found that the smaller the range that is available, *i.e.* the unpenalized space for activations, the harder it is to train the network. Intuitively, if the regularization applies too strict a constraint to activation values, the stochastic gradient descent process struggles to converge in a space full of local minima. However, a strong restriction on activation values caused detection rates to improve.

Thus when deploying models with Sitatapatra, the choice of polynomials affects base accuracies, detection rates and training time.

Key choice brings efficiency considerations to the table as well. Although training time for individual devices may be a bearable cost in many applications, a substantial increase in run-time computational cost will often be unacceptable. Table 5 reflects the total additional costs incurred by using Sitatapatra in our evaluation models. The  $< 7.5\%$  overhead we add to the base network is small, given that the models demonstrate good defence and detection rates against adversarial samples. It is notable that during inference, a detector module requires for each value  $n$  fused multiply-add operations to evaluate a  $n$ -degree  $f_k$  polynomial using Horner's method (Knuth, 1962), and 1 additional operation for threshold comparison, and thus utilize  $(n + 1)C_l H_l W_l$  operations in total for the  $l^{\text{th}}$  convolutional layer. In our evaluation, we set  $n = 2$  by using second-order polynomials. Additionally, a guard module of the  $l^{\text{th}}$  layer uses channel-wise averaging, a fully connected layer, a channel-wise scaling, and element-wise multiplications for all activations, which respectively require  $C_l H_l W_l$ ,  $C_l^2$ ,  $C_l$ , and  $C_l H_l W_l$  operations.

Model	original	detector	#FLOPs		total	overhead
			guard			
LeNet5	480,500	28,160	7,660	516,320	7.45%	
ResNet18	37,016,576	152,094	1,847,106	39,015,776	5.40%	
MCifarNet	174,301,824	715,422	646,082	175,663,328	0.64%	

Table 5. The computational costs, measured in the number of FLOPs, added by the detector and guard modules to the original network.

Polynomial	FGSM			FGSM+DeepFool+C&W		
	Precision	Recall	F1	Precision	Recall	F1
$0.1x^2 - 1x + 2 < 3$	<b>0.90</b>	<b>0.90</b>	0.90	0.81	0.29	0.43
$x^2 - 22x + 120 < 10$	<b>0.90</b>	<b>0.89</b>	0.90	<b>0.85</b>	0.28	0.42
$2x^2 + 3x + 5 < 6$	0.53	0.72	0.61	0.34	0.33	0.33
$2x^2 + 4x + 5 < 6$	0.56	0.35	0.43	0.30	0.69	0.41
Micro F1	0.72	0.72	0.72	0.40	0.40	0.40
Macro F1	<b>0.72</b>	0.72	0.71	<b>0.57</b>	0.40	0.40

Table 6. Key attribution based on the adversarial sample produced.

## 5.2. Key attribution

While exploring which activations ended up triggering an alarm with different Sitatapatra parameters, we noticed that we could often attribute the adversarial samples to the models used to generate them. In practice, this is a huge benefit, known as *traitor tracing* in the crypto research community: if somebody notices an attack, she can identify the compromised device and take appropriate action. We conducted a simple experiment to evaluate how to identify the source of a different adversarial sample. We first produced models instrumented with different polynomials using Sitatapatra and then generated the adversarial examples.

In this simple experiment, we use a support vector machine (SVM) to classify the adversarial images based on the models generated them. The SVM gets trained on the 5000 adversarial samples and gets tested on a set of 10000 unseen adversarial images. The training and test sets are disjoint.

Table 6 shows the classification results for FGSM-generated samples and all attacks combined. Precision, Recall and F1 scores are reported. In addition, we report the micro and macro aggregate values of F1 scores – micro counts the total true positive, false negatives and false positives globally, whereas macro takes label imbalance into account.

For both scenarios, we get a performance that is much better than random guessing. First, it is easier to attribute adversarial samples generated by the large coarse-grained attacks. Second, for polynomials that are different enough, the classification precision is high – for just FGSM we get a 90% recognition rate, while with more attacks it falls to 81% and 85%. For similar polynomials, we get worse performance, of around 50% for FGSM and around 30% for all combined.

This brings an additional trade-off – training a lot of different polynomials is hard, but it allows easier identification of ad-

versarial samples. This then raises the question of scalability of the Sitatapatra model instrumentation.

## 5.3. Key size

In 1883, the cryptographer Auguste Kerckhoffs enunciated a design principle that is used today: a system should withstand enemy capture, and in particular it should remain secure if everything about it, except the value of a key, becomes public knowledge (Kerckhoffs, 1883). Sitatapatra follows this principle – as long as the key is secured, it will, at a minimal cost, provide an efficient way to protect against low-cost attacks at scale. The one difference is that if an opponent secures access to a system protected with Sitatapatra, then by observing its inputs and outputs he can use standard optimisation methods to construct adversarial samples. However these samples will no longer transfer to a system with a different key.

One of the reasons why sample transferability is an unsolved problem is because it has so far been hard to generate a wide enough variety of models with enough difference between them at scale.

Sitatapatra solves this problem in principle, as it is possible to embed perhaps one key bit per channel per layer. Vision systems with hundreds of channels and dozens of layers will have enough key diversity to separate systems that are trained from scratch with entirely different keys. Whether this is a full solution to a given engineering problem will depend of whether the training overhead is acceptable.

In the case where a camera vendor wants to sell the same vision system to banks as in the mass market, it may be sufficient to have a completely independent key for the cameras sold to each bank. A training overhead of days to weeks will be entirely acceptable and will even differentiate the product. It will even be acceptable if a mass-market vendor wants to train its devices in perhaps several dozen different families, in order to stop attacks scaling (a technique adopted by some makers of pay-TV smartcards (Anderson, 2008)). However it would not be practical to have an individual key for each unit sold for a few dollars in a mass market.

Can anything be done to reduce the training overheads? We attempted to use a dynamically-rotated key in the hope that one would have to only train a single model and vary the key, but that resulted in extreme accuracy degradation.

We therefore looked for a way to speed up model generation. We developed a different training methodology (compared to Algorithm 1 on page 5 in (Shumailov et al., 2018)) and a different transfer function that is no longer dependent on activation distribution of a working model.

We can train a model to achieve high accuracy for a particular task given a small alarm rate, then start to iteratively

increase the alarm rate but decrease the learning rate. We found that the models ended up converging near the original accuracy and produce the activation values inside the range of the transfer function.

Second, we found we could fine-tune a new model based on an already instrumented one if the polynomials are not too different. We use Lagrange interpolation to generate unique polynomials with the same power as the training polynomial and that also pass through some nearby points. Polynomial similarity does however constrain the effective size of the key space, which means that attackers might find it easier to guess which polynomials a target system might use. It may also make adversarial sample attribution harder. The precise dynamics of key tweaking we leave to future work.

## 6. Conclusion

In this paper we presented Sitatapatra, a new way to use both static and dynamic channel manipulations to stop adversarial sample transfer. We show how to equip models with guards that diffuse gradients and detectors that restrict their ranges, and demonstrate the performance of this combination on CNNs of varying sizes. The detectors enable us to introduce key material as in cryptography so that adversarial samples generated on a network with one key will not transfer to a network with a different one, as activations will exceed the ranges permitted by the detectors and set off an alarm. We described the trade-offs in terms of accuracy, detection rate, and the computational overhead both for training and at run-time. The latter is about five percent, enabling Sitatapatra to work on constrained devices. The real additional cost is in training but in many applications this is perfectly acceptable. Finally, with a proper choice of transfer functions, Sitatapatra also allows adversarial sample attribution, or ‘traitor tracing’ as cryptographers call it – so that a compromised device can be identified and dealt with.

## Acknowledgements

*Partially supported with funds from Bosch-Forschungstiftung im Stifterverband.*

## References

- Anderson, R. Security engineering: a guide to building dependable distributed systems. 2008.
- Antol, S., Agrawal, A., Lu, J., Mitchell, M., Batra, D., Lawrence Zitnick, C., and Parikh, D. Vqa: Visual question answering. In *Proceedings of the IEEE international conference on computer vision*, pp. 2425–2433, 2015.
- Badrinarayanan, V., Kendall, A., and Cipolla, R. Segnet: A deep convolutional encoder-decoder architecture for image segmentation. *arXiv preprint arXiv:1511.00561*, 2015.
- Carlini, N. and Wagner, D. Towards Evaluating the Robustness of Neural Networks. In *2017 IEEE Symposium on Security and Privacy (SP)*, pp. 39–57. IEEE, 2017.
- Carlini, N., Mishra, P., Vaidya, T., Zhang, Y., Sherr, M., Shields, C., Wagner, D., and Zhou, W. Hidden Voice Commands. In *25th USENIX Security Symposium (USENIX Security 16)*. USENIX Association, 2016.
- Eykholt, K., Evtimov, I., Fernandes, E., Li, B., Rahmati, A., Xiao, C., Prakash, A., Kohno, T., and Song, D. Robust Physical-World Attacks on Deep Learning Visual Classification. In *Proceedings of the IEEE Conference on Computer Vision and Pattern Recognition*, pp. 1625–1634, 2018.
- Fang, C.-Y., Chen, S.-W., and Fuh, C.-S. Road-sign detection and tracking. *IEEE transactions on vehicular technology*, 52(5):1329–1341, 2003.
- Gao, X., Zhao, Y., Dudziak, L., Mullins, R., and zhong Xu, C. Dynamic channel pruning: Feature boosting and suppression. In *International Conference on Learning Representations*, 2019.
- Goodfellow, I. J., Shlens, J., and Szegedy, C. Explaining and harnessing adversarial examples. *International Conference on Learning Representations (ICLR)*, 2015.
- He, K., Zhang, X., Ren, S., and Sun, J. Deep residual learning for image recognition. In *Proceedings of the IEEE conference on computer vision and pattern recognition*, pp. 770–778, 2016.
- Hu, J., Shen, L., and Sun, G. Squeeze-and-excitation networks. *arXiv preprint arXiv:1709.01507*, 7, 2017.
- Ji, S., Xu, W., Yang, M., and Yu, K. 3d convolutional neural networks for human action recognition. *IEEE transactions on pattern analysis and machine intelligence*, 35(1):221–231, 2013.
- Kerckhoffs, A. La cryptographie militaire. pp. 161–191, 1883.
- Knuth, D. E. Evaluation of polynomials by computer. *Communications of the ACM*, 5(12):595–599, 1962.
- Krizhevsky, A., Sutskever, I., and Hinton, G. E. ImageNet classification with deep convolutional neural networks. In *Advances in neural information processing systems*, pp. 1097–1105, 2012.
- Krizhevsky, A., Nair, V., and Hinton, G. The CIFAR-10 dataset. 2014.



- LeCun, Y., Cortes, C., and Burges, C. MNIST handwritten digit database. 2, 2010.
- LeCun, Y. et al. LeNet-5, convolutional neural networks. pp. 20, 2015.
- Liu, X., Cheng, M., Zhang, H., and Hsieh, C.-J. Towards robust neural networks via random self-ensemble. In *European Conference on Computer Vision*, pp. 381–397, 2018.
- Liu, X., Li, Y., Wu, C., and Hsieh, C.-J. Adv-BNN: Improved Adversarial Defense through Robust Bayesian Neural Network. In *International Conference on Learning Representations*, 2019.
- Liu, Y., Chen, X., Liu, C., and Song, D. Delving into transferable adversarial examples and black-box attacks. In *International Conference on Learning Representations (ICLR)*, 2017.
- Meng, D. and Chen, H. Magnet: A two-pronged defense against adversarial examples. In *Proceedings of the 2017 ACM SIGSAC Conference on Computer and Communications Security, CCS '17*, pp. 135–147, New York, NY, USA, 2017. ACM.
- Metzen, J. H., Genewein, T., Fischer, V., and Bischoff, B. On detecting adversarial perturbations. In *Proceedings of 5th International Conference on Learning Representations (ICLR)*, 2017.
- Moosavi-Dezfooli, S., Fawzi, A., and Frossard, P. DeepFool: a simple and accurate method to fool deep neural networks. 2016.
- Papernot, N., McDaniel, P., and Goodfellow, I. Transferability in machine learning: from phenomena to black-box attacks using adversarial samples. *arXiv preprint*, 2016a.
- Papernot, N., McDaniel, P., Wu, X., Jha, S., and Swami, A. Distillation as a defense to adversarial perturbations against deep neural networks. *2016 IEEE Symposium on Security and Privacy (SP)*, May 2016b.
- Papernot, N., McDaniel, P., Goodfellow, I., Jha, S., Celik, Z. B., and Swami, A. Practical black-box attacks against machine learning. pp. 506–519, 2017.
- Ren, S., He, K., Girshick, R., and Sun, J. Faster R-CNN: Towards real-time object detection with region proposal networks. In *Advances in neural information processing systems*, pp. 91–99, 2015.
- Schroff, F., Kalenichenko, D., and Philbin, J. Facenet: A unified embedding for face recognition and clustering. In *Proceedings of the IEEE conference on computer vision and pattern recognition*, pp. 815–823, 2015.
- Shumailov, I., Zhao, Y., Mullins, R., and Anderson, R. The taboo trap: Behavioural detection of adversarial samples. *arXiv preprint arXiv:1811.07375*, 2018.
- Szegedy, C., Zaremba, W., Sutskever, I., Bruna, J., Erhan, D., Goodfellow, I. J., and Fergus, R. Intriguing properties of neural networks. *CoRR*, abs/1312.6199, 2013.
- Tsipras, D., Santurkar, S., Engstrom, L., Turner, A., and Madry, A. Robustness may be at odds with accuracy. In *International Conference on Learning Representations*, 2019.
- Yan, Z., Guo, Y., and Zhang, C. Deep defense: Training dnns with improved adversarial robustness. In Bengio, S., Wallach, H., Larochelle, H., Grauman, K., Cesa-Bianchi, N., and Garnett, R. (eds.), *Advances in Neural Information Processing Systems 31*, pp. 417–426. 2018.
- Zhao, Y., Gao, X., Mullins, R., and Xu, C. Mayo: A framework for auto-generating hardware friendly deep neural networks. 2018a.
- Zhao, Y., Shumailov, I., Mullins, R., and Anderson, R. To compress or not to compress: Understanding the interactions between adversarial attacks and neural network compression. *arXiv preprint arXiv:1810.00208*, 2018b.